Fusion Engineering and Design 123 (2017) 569–573

Contents lists available at ScienceDirect

Fusion Engineering and Design

journal homepage: www.elsevier.com/locate/fusengdes

Model-based optimal scenario planning in EAST

Hexiang Wang[a,*], Eugenio Schuster[a], Tariq Rafiq[a], Arnold Kritz[a], Siye Ding[b]

[a] Department of Mechanical Engineering and Mechanics, Lehigh University, Bethlehem, PA 18015, USA
[b] Institute of Plasma Physics, Chinese Academy of Sciences, Hefei, Anhui 230031, China

HIGHLIGHTS

- Scenario planning in EAST is formulated as a constrained nonlinear optimization problem.
- The magnetic diffusion equation is combined with physics-based correlations to obtain a control-oriented response model.
- The optimization objective is to design feedforward actuator trajectories to reach a desired plasma state.
- The desired plasma state is defined in terms of the q profile, β_N, and a stationary condition.
- The model-based optimization problem under input and state constraints is solved by employing sequential quadratic programming.

ARTICLE INFO

Article history:
Received 4 October 2016
Received in revised form 24 February 2017
Accepted 23 March 2017
Available online 7 April 2017

Keywords:
Scenario planning
Model-based control
Tokamak plasma control

ABSTRACT

Ongoing work in the fusion community focuses on developing advanced plasma scenarios characterized by high plasma confinement, magnetohydrodynamic (MHD) stability, and noninductively driven plasma current. The toroidal current density profile, or alternatively the q profile, together with the normalized beta, are often used to characterize these advanced scenarios. The development of these advanced scenarios is experimentally carried out by specifying the devices' actuator trajectory waveforms, such as the total plasma current, the plasma density, and the auxiliary heating and current-drive (H&CD) sources based on trial-and-error basis. In this work, a model-based numerical optimization approach is followed to complement the experimental effort on actuator trajectory planning in the EAST tokamak. The evolution of the q profile is closely related to the evolution of the poloidal magnetic flux profile, whose dynamics is modeled by a nonlinear partial differential equation (PDE) referred to as the magnetic-flux diffusion equation (MDE). In this work, the MDE is combined with physics-based correlations obtained from EAST experimental data for the plasma density, temperature, resistivity and non-inductive current drives to develop a control-oriented nonlinear PDE model. The optimization objective is to design feedforward trajectories for the plasma current, plasma density, electron cyclotron heating power, neutral beam injection power and lower hybrid current drive power that steer the plasma to desired q profile and β_N such that the achieved state is stationary in time. The optimization is subject to the plasma dynamics (described by the physics-based PDE model) and plasma state and actuator constraints, such as the maximum available amount of H&CD power and MHD stability limits. This defines a nonlinear, constrained optimization problem that is solved by employing sequential quadratic programming. The optimized actuator trajectories are assessed in nonlinear transport simulations in preparation for experimental tests in EAST.

1. Introduction

Extensive research has been conducted to find operating scenarios that provides high plasma performance in tokamak devices. These scenarios are characterized by high fusion gain, good plasma confinement, magnetohydrodynamic (MHD) stability and noninductively driven plasma current. Traditionally, these advanced scenarios are developed through a trial-and-error process by inputting specific actuator waveforms experimentally, such as the total plasma current and the auxiliary heating and current-drive (H&CD) powers, and analyzing the resulting plasma evolution. Two quantities often used to evaluate the operating scenario are the current density profile, or alternatively the safety factor profile (q-profile), which is related to plasma stability and performance, and

* Corresponding author.
E-mail address: hexiang@lehigh.edu (H. Wang).

http://dx.doi.org/10.1016/j.fusengdes.2017.03.143

the normalized plasma beta (β_N), which is a measure of plasma confinement [1].

One possible approach to developing an advanced operating scenario is to create a desired q-profile during the plasma current ramp-up and early flattop stages and to maintain the desired profile during the subsequent stages of the discharge. However, the desired profile may not be achievable due to physical constraints, such as the auxiliary H&CD power limit, the total plasma current ramp rate and the minimum value of the q-profile (to prevent MHD instabilities from happening and degrading the plasma performance). In practice, the goal is to achieve the best possible matching at a prespecified time during the early flattop phase of the total plasma current pulse, which defines a finite-time optimal control problem. The idea of combining predictive simulation with optimization techniques for model-based scenario planning was originally proposed in [2–5] by employing different approaches such as extremum seeking, iterative learning control, minimal surface theory and nonlinear programming. These ideas were further developed in subsequent work [6,7], where slightly different models and modified cost functions were employed. In this work, this model-based numerical optimization approach is extended to the EAST tokamak.

This paper is organized as follows. In Section 2, the poloidal magnetic flux profile and stored energy evolution models are introduced, together with a model reduction strategy. Formulation of the actuator trajectory optimization problem and its solution is given in Section 3. Test result showing the effectiveness of the optimized trajectory is presented in Section 4. In Section 5 conclusions and future work are presented.

2. Poloidal flux and stored energy evolution models

Any quantity constant on each magnetic surface could be chosen as an indexing coordinate ρ. We choose the mean effective minor radius of the magnetic surface as the variable ρ, i.e., $\pi B_{\phi,0}\rho^2 = \Phi$, where Φ is the toroidal magnetic flux and $B_{\phi,0}$ is the toroidal magnetic field at the major radius of the device, R_0. The normalized effective minor radius $\hat{\rho}$ is defined as $\hat{\rho} = \rho/\rho_b$, where ρ_b is the mean effective minor radius of the uttermost closed magnetic flux surface. The evolution of the poloidal magnetic flux is given by the magnetic diffusion equation (MDE) [8]

$$\frac{\partial \psi}{\partial t} = \frac{\eta(T_e)}{\mu_0 \rho_b^2 \hat{F}^2}\frac{1}{\hat{\rho}}\frac{\partial}{\partial \hat{\rho}}\left(\hat{\rho} D_\psi \frac{\partial \psi}{\partial \hat{\rho}}\right) + R_0 \hat{H}\eta(T_e)\frac{\langle \bar{j}_{NI}\cdot \bar{B}\rangle}{B_{\phi,0}}, \tag{1}$$

where ψ is the poloidal flux per radian, which is closely related to the poloidal flux Ψ, i.e. $\Psi = 2\pi\psi$, t is the time, η is the plasma resistivity, T_e is the electron temperature, μ_0 is the vacuum permeability, $\bar{j}_{NI}$ is any source of noninductive current density, $\bar{B}$ is the magnetic field, $\langle\rangle$ denotes a flux-surface average, and $D_\psi(\hat{\rho}) = \hat{F}(\hat{\rho})\hat{G}(\hat{\rho})\hat{H}(\hat{\rho})$. The parameters $\hat{F}(\hat{\rho})$, $\hat{G}(\hat{\rho})$, $\hat{H}(\hat{\rho})$ are geometric factors pertaining to the magnetic configuration of a particular fixed plasma equilibrium. The boundary conditions are given by

$$\left.\frac{\partial \psi}{\partial \hat{\rho}}\right|_{\hat{\rho}=0} = 0 \qquad \left.\frac{\partial \psi}{\partial \hat{\rho}}\right|_{\hat{\rho}=1} = -\frac{\mu_0}{2\pi}\frac{R_0}{\hat{G}(1)\hat{H}(1)} I_p(t), \tag{2}$$

where $I_p(t)$ is the total plasma current.

The volume-averaged plasma energy balance can be described as

$$\frac{dE}{dt} = -\frac{E}{\tau_E(t)} + P_{tot}(t), \tag{3}$$

where τ_E is the global energy confinement time and P_{tot} is the total power injected into the plasma, which can be represented as $P_{tot}(t) = P_{ohm}(t) + P_{nbi_1}(t) + P_{nbi_2}(t) + P_{lh}(t) + P_{ich}(t) - P_{rad}(t)$. $P_{ohm}(t)$ is the ohmic power, $P_{nbi_1}(t)$ and $P_{nbi_2}(t)$ are the powers of the two neutral beam injectors, $P_{lh}(t)$ is the power of the lower hybrid wave launcher, $P_{ich}(t)$ is the powers of the ion cyclotron, and $P_{rad}(t)$ is the radiated power. The energy confinement time τ_E is modeled as [9]

$$\tau_E(t) = 0.023 I_p^{0.96} P_{tot}^{-0.73} R_0^{1.89} a^{-0.06} \bar{n}_e^{0.40} B_{\phi,0}^{0.03} A_{eff}^{0.20} \kappa^{0.64}, \tag{4}$$

where a is the minor radius, $\bar{n}_e$ is the line average density, A_{eff} is the average ion mass and κ is the elongation.

2.1. Plasma parameters

Some plasma parameters that are of interest in determining the stability and performance of a tokamak are taken into consideration for actuator trajectory planning, such as the q-profile, the plasma β_N and the plasma loop-voltage profile U_p. The q-profile is related to the spatial gradient of the poloidal magnetic flux and is defined as

$$q(\hat{\rho}, t) = -\frac{d\Phi}{d\Psi} = -\frac{B_{\phi,0}\rho_b^2\hat{\rho}}{\partial\psi/\partial\hat{\rho}}. \tag{5}$$

The plasma β_N is related to the volume-averaged plasma stored energy E and is defined as

$$\beta_N = \beta_t[\%]\frac{aB_{\phi,0}}{I_p}, \quad \beta_t = \frac{\langle p\rangle_V}{B_{\phi,0}^2/(2\mu_0)} = \frac{2E/V_p}{3B_{\phi,0}^2/(2\mu_0)}, \tag{6}$$

where β_t is the plasma toroidal beta, p is the plasma kinetic pressure, and V_p is the total plasma volume. The loop-voltage profile is related to the temporal derivative of the poloidal magnetic flux and is defined as

$$U_p(\hat{\rho}, t) = -2\pi\frac{\partial\psi}{\partial t}. \tag{7}$$

2.2. Model reduction via finite difference

To simulate the infinite dimensional PDE (1)–(2), the spatial domain is discretized via a finite-difference method. By defining the vector state $Z = [\psi(\hat{\rho}_i, t), E(t)]$, for $i = [1, 2, \ldots, n-1, n]$, where n is the number of points in the spatial grid, an augmented system which combines (1)–(2) and (3) is written as

$$\dot{Z} = F(Z, u), \tag{8}$$

where u are the system inputs (defined in next section).

3. Actuator trajectory optimization problem

The goal of the actuator trajectory optimization problem is to determine feedforward actuator waveforms that drive the plasma to a target state (defined in terms of the q-profile ($q^{tar}(\hat{\rho})$) and normalized plasma beta (β_N^{tar})) at some time t_f during the early flattop stage of plasma discharge in such a way that the achieved state is as stationary in time as possible.

3.1. Cost function definition

As the poloidal flux profile evolves with the slowest time constant in the plasma, if it reaches a stationary condition, i.e., $U_p(\hat{\rho}, t)$ = constant, all of the other plasma profiles have also reached a stationary condition. Therefore, the stationarity of the plasma state can be defined by the profile $g_{ss}(\hat{\rho}, t) = 0$, where $g_{ss}(\hat{\rho}, t) = \partial U_p/\partial\hat{\rho}$. The proximity of the achieved plasma state to the target state at the time t_f can be described by the cost function

$$J(t_f) = k_{ss}J_{ss}(t_f) + k_q J_q(t_f) + k_{\beta_N} J_{\beta_N}(t_f), \tag{9}$$

where k_{ss}, k_q, k_{β_N} are used to weight the relative importance of the plasma state characteristics, and J_{ss}, J_q, J_{β_N} are defined as

$$J_{ss}(t_f) = \int_0^1 W_{ss}(\hat{\rho})[g_{ss}(\hat{\rho}, t_f)]^2 \, d\hat{\rho}, \tag{10}$$

$$J_q(t_f) = \int_0^1 W_q(\hat{\rho})[q^{tar}(\hat{\rho}) - q(\hat{\rho}, t_f)]^2 \, d\hat{\rho}, \tag{11}$$

$$J_{\beta_N}(t_f) = [\beta_N^{tar} - \beta_N(t_f)]^2, \tag{12}$$

where $W_q(\hat{\rho})$ and $W_{ss}(\hat{\rho})$ are positive functions used to weight which portions of the respective profiles are more important relative to the others.

3.2. Actuator constraints and parameterization

The actuators are two neutral beam injectors (NBI), one lower hybrid (LH) wave launcher, one ion cyclotron (IC) wave launcher, the total plasma current I_p and the line average electron density u_n. In this work, the line average electron density is considered as a measurable quantity instead of as an actuator due to its associated control challenges. The actuator magnitude and rate constraints are given by

$$I_p^{\min} \le I_p(t) \le I_p^{\max}, \tag{13}$$

$$P_{nbi1}^{\min} \le P_{nbi1} \le P_{nbi1}^{\max}, \tag{14}$$

$$P_{nbi2}^{\min} \le P_{nbi2} \le P_{nbi2}^{\max}, \tag{15}$$

$$P_{lh}^{\min} \le P_{lh} \le P_{lh}^{\max}, \tag{16}$$

$$P_{ic}^{\min} \le P_{ic} \le P_{ic}^{\max}, \tag{17}$$

$$-I_{p,\max}^{d} \le dI_p/dt \le I_{p,\max}^{u}, \tag{18}$$

where $(\cdot)^{min}$ and $(\cdot)^{max}$ are the minimum and maximum limits, respectively, and $I_{p,\max}^{d}$ and $I_{p,\max}^{u}$ are the maximum total plasma current ramp-down and ramp-up rates, respectively. P_i, where $i \in \{nbi1, nbi2, lh, ic\}$, is the individual power input from different actuators. By defining the control input vector $u = [P_{nbi1}, P_{nbi2}, P_{lh}, P_{ic}, I_p]$, we could parameterize the trajectory of the ith control actuator (u_i) by a finite number of parameters (n_{u_i}) at discrete points in time (t_{u_i}), i.e., $t_{u_i} = [t_i^0, t_i^1, \ldots, t_i^k, \ldots, t_i^{(n_{u_i}-2)}, t_i^{(n_{u_i}-1)} = t_f]$ for $i \in [1, 5]$, $k \in \{0, 1, 2, \ldots, n_{u_i} - 1\}$. By combining all of the parameters into a vector $\theta = [u_1^1, \ldots, u_1^{n_{u_1}}, \ldots, u_i^1, \ldots, u_i^{n_{u_i}}, \ldots, u_5^1, \ldots, u_5^{n_{u_5}}]$, the actuator trajectories can be obtained by interpolation of θ, i.e., $u_i(t) = u_i(t_i^k) + (u_i^{k+1} - u_i^k)(t - t_i^k)/(t_i^{k+1} - t_i^k)$ for $t \in [t_i^k, t_i^{k+1}]$. The actuator constraints (13)–(18) can be written in matrix form as

$$A_u^{\lim}\theta \le b_u^{\lim}. \tag{19}$$

3.3. Magnetohydrodynamic (MHD) stability constraints

The first MHD-related stability limit considered in this work is expressed as

$$q_{\min}(t) \ge q_{\min}^{\lim}, \tag{20}$$

where $q_{\min}(t) = \min(q(\hat{\rho}, t))$ and $q_{\min}^{\lim}$ is a constant chosen to be slightly greater than one to avoid the onset of sawtooth oscillations. The next MHD-related stability limit considered in this work is given by

$$\bar{n}_{e20}(t) \le n_g(t), \tag{21}$$

where $\bar{n}_{e20}(t)$ is the line-averaged electron density evaluated in units of $10^{20}\,\mathrm{m}^{-3}$ and $n_g(t) = I_p(t)[MA]/\pi a^2$ is referred to as the Greenwald density limit. The last MHD-related constraint considered in this work is given by

$$\beta_N(t) \le \beta_N^{\lim}. \tag{22}$$

To reduce the computational burden, these three MHD constraints are then formulated into one integral constraint,

$$c_{MHD}^{\lim}(Z) \le 0, \tag{23}$$

where

$$c_{MHD}^{\lim}(Z) = \int_{t_0}^{t_f} \Big[\max\{0, q_{\min}^{\lim} - q_{\min}(t)\} + \max\{0, \bar{n}_{e20}(t) - n_g(t)\} + \max\{0, \beta_N(t) - \beta_N^{\lim}\}\Big] \, dt. \tag{24}$$

3.4. Optimization problem statement and solution method

By following the steps in previous section, the actuator trajectory planning can be formulated as an optimization problem,

$$\min_{\theta} J(t_f) = J(\dot{Z}(t_f), Z(t_f)), \tag{25}$$

subject to equality (8) and inequalities (19) and (23).

We apply sequential quadratic programming (SQP) to solve this optimization problem. The idea of SQP is to approximate the cost function by a second order Taylor expansion and the constraints by a first order Taylor expansion at the current iteration's solution. This defines a quadratic optimization problem that can be solved by quadratic programming to obtain a new solution. This iterative process continues until certain criteria are met.

4. Simulation tests of optimized actuator trajectories

The optimization is carried out over the time interval $t_{opt} = [t_0, t_f] = [1, 2.9]$ for four different cost functions characterized by the following weights:

Case1 : $k_{ss} = 1,\ k_q = 100,\ k_{\beta_N} = 1;$

Case2 : $k_{ss} = 1,\ k_q = 1,\ k_{\beta_N} = 100;$

Case3 : $k_{ss} = 100,\ k_q = 1,\ k_{\beta_N} = 1;$

Case4 : $k_{ss} = 50,\ k_q = 10,\ k_{\beta_N} = 5.$

All the actuator values at the initial time t_0 are fixed. The ion cyclotron in this work is not optimized. Instead, a suitable ion cyclotron power evolution is extracted from experiments relevant to the scenario of interest. The vector of to-be-optimized parameters is then given by

$$\begin{aligned} \theta = \ & [P_{nbi1}(1.5), P_{nbi1}(2), P_{nbi1}(2.5), P_{nbi1}(2.9), P_{nbi2}(1.5), \\ & P_{nbi2}(2), P_{nbi2}(2.5), P_{nbi2}(2.9), P_{lh}(1.5), P_{lh}(2), \\ & P_{lh}(2.5), P_{lh}(2.9), I_p(1.5), I_p(2.9)]. \end{aligned} \tag{26}$$

The optimized actuator trajectories and constraints are shown in Fig. 1. It can be seen that no constraint is violated. The optimized actuator trajectories are tested through simulations using the model proposed in Section 2. The comparisons between the target profiles and model-predicted profiles based on the optimized actuator trajectories are shown in Fig. 2. It can be seen from the figure that β_N is well below $\beta_N^{\lim}$, which is set to 2 in this optimization. Also, it can be seen that under the same actuator constraints, the q and β_N evolutions are sensitive to the selected weights in the cost function. Besides weight selection, the outcome of the optimization procedure depends heavily on the quality of the prediction model and the chosen actuator parameterization.

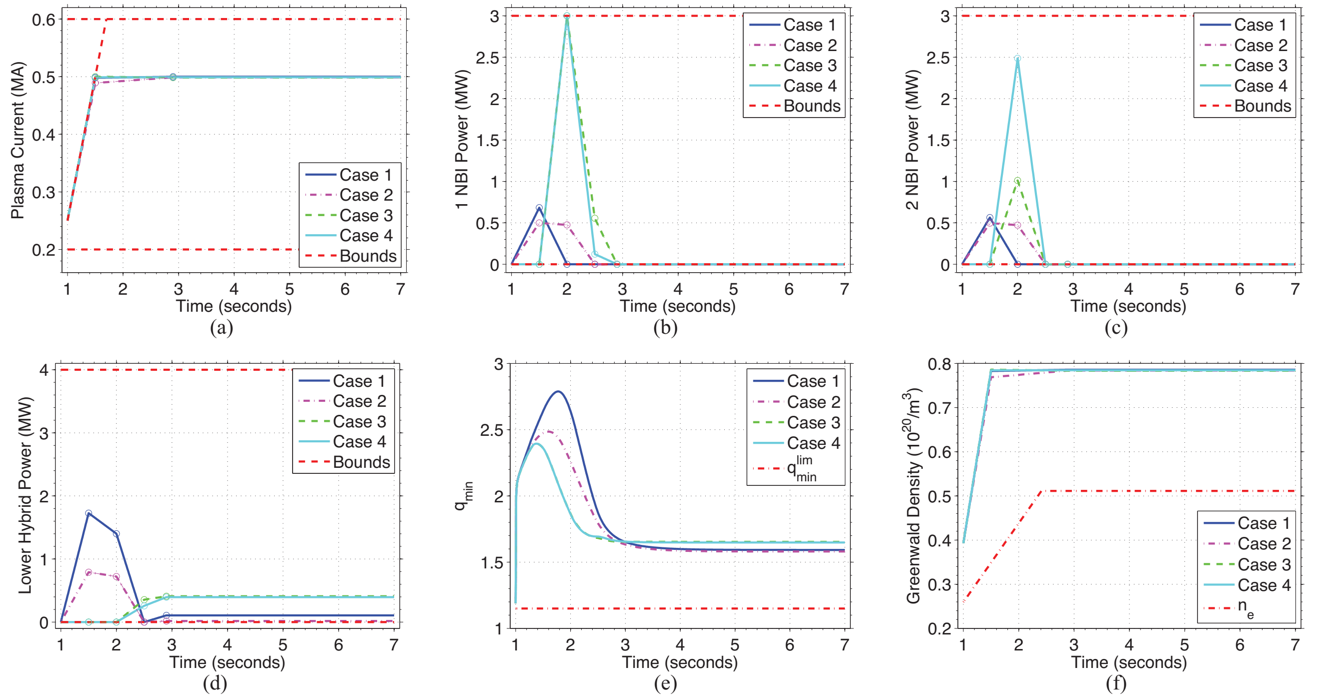

Fig. 1. Optimized actuator trajectories and physical constraints: (a) total plasma current, (b) first NBI power, (c) second NBI power, (d) lower hybrid wave power, (e) q_{min} vs. q_{min}^{lim}, and (f) Greenwald density constraints vs. $\bar{n}_e$ (note that the same $\bar{n}_e$ is prescribed for all cases).

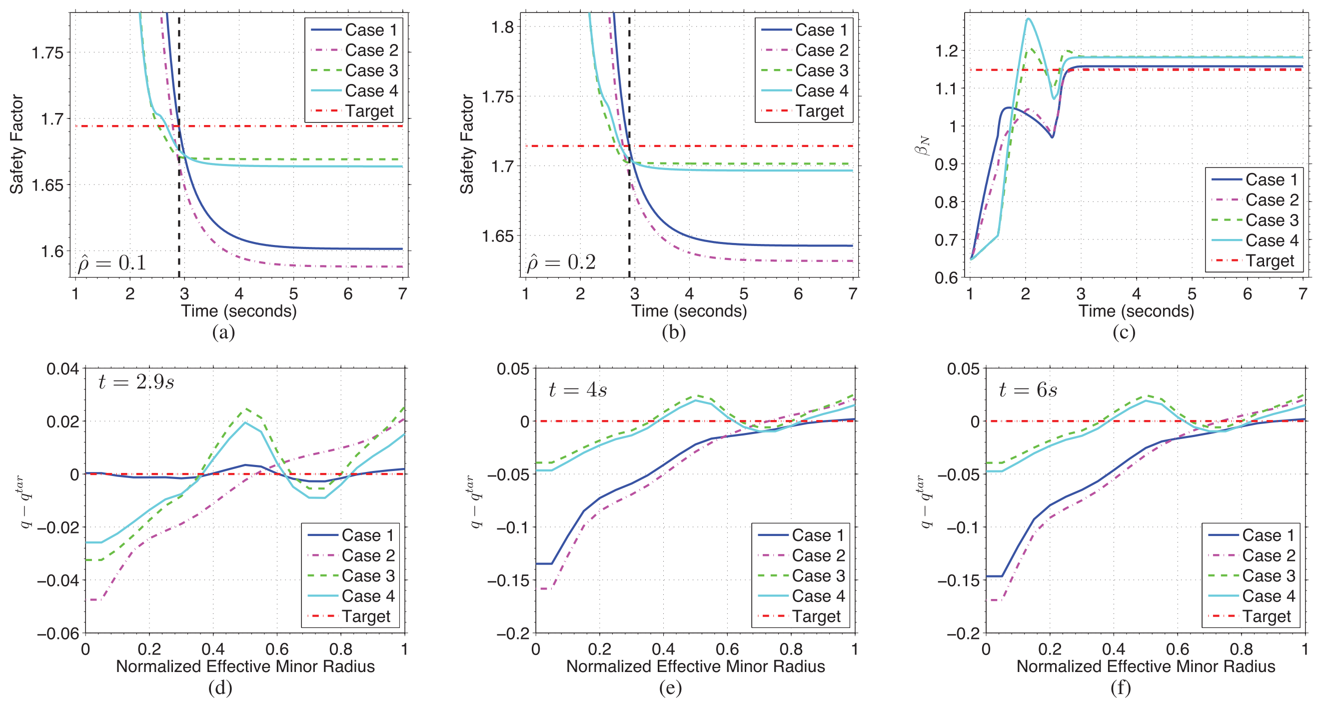

Fig. 2. Simulation-based testing of optimized actuator trajectories: (a and b) time evolution of q in the plasma core ($\hat{\rho} = 0.1$ and $\hat{\rho} = 0.2$), (c) evolution of β_N, and (d–f) difference between actual and target q-profiles at different times.

5. Conclusions and future work

In this paper, a model-based actuator trajectory optimization problem has been formulated and solved by applying sequential quadratic programming. The optimized actuator trajectories have been successfully tested in simulations. Our future work includes experimental testing of the optimized actuator trajectories in EAST, followed by an assessment on the need of refining the prediction model. The use of a heat transport equation could be evaluated as a means of improving the model accuracy. However, the design of optimized feedforward trajectories does not take into account mismatches between the plasma system and the model, which is never perfect. Moreover, unpredictable disturbances can affect the plasma in real time. Therefore, in practice the feedforward control solution always need to be complemented by a feedback controller [7].

Acknowledgments

Work supported by the U.S. Department of Energy (DE-SC0010537).

References

[1] J. Wesson, Tokamaks, Clarendon Press, Oxford, 2004.
[2] Y. Ou, C. Xu, E. Schuster, et al., Design and simulation of extremum-seeking open-loop optimal control of current profile in the DIII-D tokamak, Plasma Phys. Control. Fusion 50 (2008) 115001.
[3] C. Xu, R. Arastoo, E. Schuster, On iterative learning control of parabolic distributed parameter systems, in: Proceedings of the 17th Mediterranean Conference on Control and Automation, Thessaloniki, Greece, 2009.
[4] C. Xu, E. Schuster, Control of ramp-up current profile dynamics in tokamak plasmas via the minimal-surface theory, in: Proceedings of the 48th IEEE Conference on Decision and Control, Shanghai, China, 2009.
[5] C. Xu, J. Dalessio, Y. Ou, E. Schuster, et al., Ramp-up phase current profile control of tokamak plasmas via nonlinear programming, IEEE Trans. Plasma Sci. 38 (2) (2010) 163–173.
[6] F. Felici, O. Sauter, Non-linear model-based optimization of actuator trajectories for tokamak plasma profile control, Plasma Phys. Control. Fusion 54 (2012) 025002.
[7] J. Barton, M. Boyer, W. Shi, W. Wehner, E. Schuster, et al., Physics-model-based nonlinear actuator trajectory optimization and safety factor profile feedback control for advanced scenario development in DIII-D, Nuclear Fusion 55 (9) (2015) 093005.
[8] Y. Ou, T.C. Luce, E. Schuster, et al., Towards model-based current profile control at DIII-D, Fusion Eng. Des. 82 (2007) 1153–1160.
[9] M. Wakatani, et al., ITER physics basis, Nuclear Fusion 39 (12) (1999) 2201–2206.